Ab Initio Frequency Calculations of Pyridine Adsorbed on an Adatom Model of a SERS Active Site of a Silver Surface

Alberto Vivoni,*,† Ronald L. Birke,*,‡ Richard Foucault,‡ and John R. Lombardi‡

Department of Biology, Chemistry and Environmental Sciences, Inter American University, San Germán Campus, San Germán PR 00683, Puerto Rico, and The City College and The Graduate School and University Center of the City University of New York, Department of Chemistry and Center for Analysis of Structures and Interfaces (CASI), New York, New York 10031

Received: December 6, 2002; In Final Form: March 31, 2003

Ab initio and Urey−Bradley calculations of normal modes were carried out to analyze the frequency shifts observed on the SERS spectrum of pyridine obtained on a Ag surface. A molecular model with a Ag atom attached to the pyridine nitrogen was used in the Urey−Bradley calculation. The frequency shifts in the SERS spectrum were calculated by adding K(Ag−N) and F(Ag···C_α) force constants and by adjusting the ring stretches according to how their bond lengths changed in an ab initio calculation with a $(Ag-Py)^+$ model. The ab initio calculations were done with the HF, MP2, and B3LYP methods using the 3-21G, 6-31G, 6-31G*, 6-31G**, and LanL2DZ basis sets. The surface active site was modeled in the calculation by means of Ag^0, Ag^+ atoms, and a Ag_4^+ pyramidal cluster structure. The calculations were evaluated on how well they matched the observed frequencies, the ν(Ag−N) stretch, and the frequency shifts for the SERS spectrum in an electrochemical environment. The calculation with the Ag_4^+ model yielded the best results although the $(Ag-Py)^+$ model also gives reasonable results. All calculations were consistent with an edge-on interaction between pyridine and the electrode surface and a Ag^+ species as part of the surface active site.

Introduction

Since the first measurements by Fleischman et al. in 1974,[1] surface enhanced Raman scattering (SERS) spectroscopy has become a powerful technique for studying the vibrational properties and structure of molecules on SERS active metal surfaces and a powerful tool for chemical analysis of molecules which can be coupled to such surfaces. Indeed, the technique has generated a great deal of interest recently, having been used to obtain single molecule Raman spectroscopy (see recent reviews[2]) as well as the Raman spectra of molecules adsorbed on nanoparticles,[3] to study self-assembled monolayers,[4] as probe for trace environmental analysis,[5] and as a tracer for DNA and RNA detection,[6] to cite a few examples of topical applications. Despite the widespread use of SERS, relatively few ab initio theoretical studies have been made to elucidate the effect on the SERS vibrational spectra of the molecular interaction between the adsorbate molecule and the metal substrate. It is well-known that the so-called chemical enhancement mechanism of SERS, which we believe is essential for observing a SERS spectrum, requires a bonding interaction between the metal substrate and the adsorbed molecule.[7] In principle, these theoretical studies could provide the relationship between the molecular level properties of the interfacial structure and the SERS process, which in turn could help in the use of SERS spectra to elucidate such properties as the orientation of molecules on various surface sites, the type and strength of the bonds between the molecule and the surface, the reasons for frequency shifts observed with surface adsorbed molecules, the nature of the surface roughness on the atomic scale, and the very nature of the chemical enhancement mechanism itself.

Herein, we use ab initio molecular orbital calculations for a pyridine−Ag metal cluster system as a theoretical approach to investigate some these problems, especially the effect of the bonding interaction at the Ag surface on the band positions of the SERS spectrum of pyridine. Molecular orbital metal cluster−molecule studies have been used to investigate metal to ligand chemical bonding in small metal cluster−ligand systems such as Ag_n-L[8,9] or Cu_n-L,[10,11] where $n = 1-18$, to model binding on M(100), M(111), and M(110) metal surfaces. The ligand−metal adsorption geometries investigated were the on-top site where the ligand is directly above a single metal atom, the bridging site where the ligand is directly above a dimer of two metal atoms in the surface, and the hollow site where the ligand is directly above a triangle formed by three metal atoms in the surfaces.[8−11]

To postulate a chemical model for the molecular orbital frequency calculations, we need to consider the experimental evidence for the structure of the metal−molecule system. A very interesting early paper where pyridine was cocondensed with Ag_2 and Ag_3 in a solid argon matrix[12] showed a set of vibrational frequencies very similar to the SERS spectrum of pyridine from a Ag electrode in the potential region of −0.2 to −0.6 V versus SCE. In fact, a 242 cm^{-1} band in the matrix isolation spectrum was assigned to the Ag−N stretch, as is usually done for the SERS of pyridine on a Ag surface.[13] In fact, Creighton et al.[14] assigned the ∼239 cm^{-1} band to a ν(Ag−N) mode because it also showed up in the spectrum of metal−pyridine complexes. However, various other authors claimed that the band was due to a Ag−Cl^- stretch.[15,16] We showed that the 239 cm^{-1} band still appears in Cl^- free solution SERS spectra of pyridine and various pyridine derivatives adsorbed on Ag sols.[13] Similar

* To whom correspondence should be addressed by e-mail: A.V., avivoni@sg.inter.edu; R.L.B., birke@sci.ccny.cuny.edu.

† Inter American University.

‡ The City College of the City University of New York.

10.1021/jp027642o CCC: $25.00
Published on Web 05/16/2003

results were obtained by Neto et al. for bipyrazine[17] also adsorbed on Ag sols. These authors found that the addition of Cl^- ions to the silver sols produced a strong ν(Ag−Cl) band that "masked" the ν(Ag−N) vibration. Furthermore, Muniz-Miranda et al.[18] found from potential dependence experiments on a Ag electrode that, at −0.6 V versus SCE, the Cl^- ion desorbs from the surface and that a ν(Ag−N) stretch is still observed at 220 cm^{-1}. In all, these results show that, in the presence of Cl^- ions, the 239 cm^{-1} band must have at least partially a ν(Ag−N) stretching contribution. This surface-molecule vibration is thus taken as evidence for the edge-on interaction of the pyridine nitrogen with surface Ag.

Of course, for the roughened metal surface the pyridine molecule orientation has been discussed as either edge-on or face-on with respect to a microsized Ag particle.[19,20,21] The edge-on binding in an on-top site is predicted to occur by the mostly nitrogen σ-donor orbital, $7a_1$ (σ), of pyridine interacting with vacant Ag (5s, $5p_z$) orbitals while edge-on binding in a bridge-site occurs more through the π-donor pyridine orbital, $2b_1$, interacting with Ag orbitals.[9] This type of binding should align the molecular axis of pyridine either at a right angle with respect to the extended surface or at an inclined angle. The face-on binding would occur through the $1a_2$ (π) HOMO orbital of the aromatic ring. This type of binding is expected to align the molecular axis and the molecular plane of pyridine parallel to the Ag surface.

However, various experimental techniques such as angle-resolved ultraviolet photoelectron spectroscopy (ARUPS) and near-edge X-ray absorption fine structure (NEXRAFS) indicate that pyridine bonds to Ag, Cu, and Pt surfaces through the nitrogen lone-pair electrons either in a perpendicular manner to the surface or slightly tilted.[22,23] The discussion of the orientation of molecules observed by SERS on a roughened surface is somewhat confusing, since it should depend on whether the orientation is with respect to an atomic scale site or the microcrystalline surface particles created by the roughening procedure. A comparison of the frequency shifts in the SERS spectrum with those in the spectrum of a pyridine−Ag ion complex suggests that the molecule bonds to the SERS active surface in the same way that it bonds when coordinating to a Ag ion, that is, edge-on through the nitrogen atom.[14]

On the other hand, Creighton[19] later found through the use of the small isolated sphere electromagnetic (EM) surface enhancement rules of SERS that the molecule should be flat on the surface at an electrode potential of −0.5 V versus SCE. We also used the EM selection rules[7,24] for pyridine bands as a function of potential to conclude that the molecule lies flat on the surface at −0.6 V versus SCE, in agreement with Creighton's results, but that it stands up at −0.9 V. In another study, a theoretical analysis of intensity ratios based on the Pariser, Parr, and Pople semiempirical method in the surface enhanced hyper-Raman spectrum of pyridine[25] showed that pyridine is already standing up at −0.7 V versus SCE. In fact, it is easy to appreciate that the results from the use of the EM selection rules do not give information about the binding geometry at the atomic Ag sites. If the active site is a small Ag cluster on the Ag surface, the pyridine could be bound to a Ag cluster edge-on and still be in a parallel orientation with respect to the microsized Ag particles, which gives rise to the EM selection rules. In fact, Creighton concluded that σ-bonded pyridine is not incompatible with a parallel orientation to the roughened Ag surface.[19]

Despite the difficulties in probing the roughened metal surface for atomic scale details, some SERS experimental results indicate that interaction between pyridine and a silver surface occurs through a metal adatom. By analyzing the SERS spectrum of cyanide under various conditions during the oxidation−reduction cycle (ORC) pretreatment, Billman et al. found that the signal enhancement occurred after the formation of a silver surface that was rough on an atomic scale.[26] They thus concluded that the surface−adsorbate interaction occurred through an adatom on the surface. SERS experiments by Bunding et al. in our laboratory with 2,6-dimethylpyridine (lutidine) supported this conclusion.[27] This molecule has its two methyl groups on α carbons to the nitrogen that restricts the interaction with the surface to a single metal atom; yet, a SERS enhancement is still observed, providing evidence that the interaction with the surface adatom does occur. Roy and Furtak[28] went further and proposed that the active site was made up of a Ag_4^+ pyramidal cluster. These authors arrived at this proposition by associating some low-frequency vibrations in the SERS spectra with Ag−Ag stretching modes of the pyramidal cluster. This model is consistent with the direct interaction of the scattering molecule with a nearest neighbor adatom, since an adatom in this cluster would sit on top of three other Ag atoms that form the base of the pyramid.

Various theoretical models for calculating SERS spectral frequencies have been previously studied involving ab initio methods for the molecule interacting with a metal surface. Recently, Corni and Tomasi treated the molecule at the ab initio level whereas the surface was treated by the dielectric properties of a continuous metallic body and by the polarizable dipoles of spherical metallic particles.[29,30,31] Other authors have represented the surface through various metal adatom or small metal cluster models. Kwon et al. used a planar Ag_5^+ model with four Ag atoms at the corner of a square and a fifth one at the center with frozen bulk distances to model the energetics for perpendicular and flat orientations of benzoic acid using the LanL1DZ basis set.[32] Cardini and Muniz-Miranda[33] used two Ag atoms at different positions of a pyrazole structure and performed density functional theory, DFT, calculations of the frequencies for pyrazole bonded to silver atoms using a mixed 6-31G(d)/LanL2DZ basis set. Arenas et al.[34] represented a Ag surface by two metal atoms aligned along the molecular axis of pyrazine, using the LanL2DZ basis set and the RHF and CIS level methods to calculate ground- and excited-state energies and frequencies. SERS spectral bands have also been calculated by Vivoni et al.[35] using the model of a single Ag^+-6-mercaptopurine complex bonded edge-on (semiempirical PM3 method), while Acoca et al.[36] modeled the SERS spectra for the phthalimide $-Ag^+$ complex with Hartree−Fock and DFT(S−VWN) theory with the LanL2DZ basis set.

All things considered, there have been relatively few ab initio frequency calculations of SERS spectra where the effect of the metal binding site has been explicitly included in the calculation. In fact, even though pyridine was the first molecule whose SERS spectrum was observed,[1] there are no ab initio calculations in the literature with a Ag atom or cluster included in the chemical model of the scattering species, although ab initio calculations of the pyridine SERS spectrum have been carried out without explicitly involving the Ag metal.[37] The results cited above from (i) matrix isolation spectroscopy,[12] (ii) evidence for adatom involvement,[26,27] and (iii) the low-frequency Ag vibrations identified by Roy and Furtak[28] provide good evidence that a small Ag cluster model should be a very adequate representation of the SERS active site for pyridine on a Ag surface. We will also present evidence from empirical normal mode calculations

TABLE 1: UBFF Force Constants of Pyridine, in mdyn/Å, Obtained by Fitting the Gas Phase Frequencies and Their Modification To Fit the SERS Frequencies

force constant type[a]	gas phase	SERS
K(N1C2)	5.58	5.48
K(C2C3)	4.94	5.14
K(C3C4)	4.72	4.72
K(Ag−N)		1.10
H(−CH)	0.33	0.33
H(−C−)	0.82	0.82
H(−N−)	0.28	0.10
ρ	0.37	0.37
F(C···C)	0.72	0.72
F(N···C)	0.38	0.38
F(C···H)	0.38	0.38
F(N···H)	0.59	0.59
F(Ag···C_α)		0.40

[a] K = bond stretch, H = angle bend, F = nonbonded interaction, ρ = aromatic interaction

that the SERS spectrum of pyridine is consistent with pyridine binding edge-on to a Ag adatom site on the surface.

We have calculated the vibrational frequency shifts of pyridine bonded to silver using both a Urey−Bradly empirical force field and ab initio methods. Recently, various authors have calculated with empirical force fields the differences in vibrational frequencies (or vibrational frequency shifts) between free molecule and surface-enhanced Raman scattering (SERS) spectra by modeling the surface in SERS through metal atoms. Neto et al.[17] carried out this kind of calculation with bipyrazine, Muniz-Miranda with 1,10-phenanthroline,[38] and Vivoni et al. with 6-mercaptopurine.[35] For the ab initio calculations of the effect of the metal (Ag) on SERS spectra of pyridine, we use a model with an on-top geometry site, the model systems being Ag−pyridine, Ag^+−pyridine, and Ag_4^+−pyridine with the pyridine nitrogen directed at a single Ag adatom. The goal of our ab initio calculations is to obtain a method that is not too computationally expensive but that yields satisfactory results when compared to experiment. Hartree−Fock and DFT calculations are evaluated according to how well they predict the ν(Ag−N) mode at 239 cm^{-1} and how well they match the frequency shifts on going from a gas phase spectrum of pyridine to the SERS spectrum of pyridine. Initially, normal mode calculations were done with a neutral silver atom−pyridine (Ag−Py) model. But those calculations yielded a ν(Ag−N) mode that was too low. Ab initio calculations with a $(Ag-Py)^+$ model yielded a ν(Ag−N) mode higher than that of the neutral model, but they are still short of the experimental value. Finally, we obtained a closer value by carrying out a calculation with the Ag_4^+ cluster model, $(Ag_4-Py)^+$, that Roy and Furtak proposed for the active site on the surface.[28]

Calculation Methods

We performed two types of calculations for this work: Urey−Bradley force field (UBFF) and ab initio calculations. The UBFF calculations were carried out using the Diem version of Schachtshneider PC programs adapted for a SIMPLEX refinement of the force constants.[39,40] The calculation of the free pyridine force field was discussed in ref 39. Basically, it consisted of reducing the number of diagonal force constants by treating all angle bends with the same center atom as equal. The number of nonbonded force constants was reduced in a similar manner by treating all nonbonded interactions that had the same corner atoms as equal. The resulting force field, shown in Table 1, had 12 force constants: seven diagonal interactions, four nonbonded interactions, and the aromatic interaction, ρ. These force constants were refined by fitting the gas-phase spectra of two isotopomers: pyridine-h_5 and pyridine-d_5. The force field thus obtained was checked against the spectra of four others isotopomers. It reproduced a total of 152 experimental frequencies with an average error of 0.68%. In the present work, we used this force field in order to reproduce the vibrational frequency shifts observed in the SERS spectrum.

Following the Suzuki and Orville−Thomas calculation model,[41] we added to the pyridine force field a K(Ag−N) stretching force constant and a F(Ag···C_α) nonbonded interaction. The silver atom was placed at 2.3 Å from the nitrogen along the molecular axis, thus retaining the C_{2v} symmetry. This is the Ag^+−N bond length in the X-ray crystal structure of tetrahedral $[Ag(Pyd)_4]ClO_4$.[42] The K(Ag−N) and F(Ag···C_α) force constants were adjusted at 1.10 and 0.40 mdyn/Å, respectively, such as to match the 239 cm^{-1} band and the vibrational frequency shift of the totally symmetric ring breathing (mode 1) that occurs at 991 cm^{-1} in the gaseous spectrum. The shift of this normal mode is the second largest in the SERS spectrum. The ring force constants were adjusted according to the changes in bond length obtained from a UHF/3-21G calculation that will be described in the next paragraph. The gaseous phase frequencies used were from the results of Stidham and DiLella,[43] and the SERS frequencies were from those found by Creighton,[19] which came from a Ag electrode system at −0.5 V versus SCE.

The ab initio calculations were done with the 94 and 98 versions of Gaussian.[44] Initial calculations were carried out with the UHF/3-21G method with the free pyridine molecule and with an Ag atom bonded to nitrogen. These initial calculations were done with neutral and +1 charged models and yielded frequency differences between a gas phase model and an $(Ag-Py)^+$ model which we associated with the frequency shifts observed in the SERS spectrum. From these calculations we also obtained the changes in bond lengths that were used to adjust the force constants in the UBFF calculation in order to match the vibrational frequency shifts not accounted for by the addition of the K(Ag−N) and F(Ag···C_α) force constants. Subsequent ab initio calculations were done for free pyridine with the Hartree−Fock method using the 6-31G, 6-31G*, and 6-31G** basis sets, with the MP2 method using the 6-31G** and LanL2DZ basis sets, and with the B3LYP method using the LanL2DZ basis set. For calculations including Ag, we compared the 3-21G with the LanL2DZ basis set. Each frequency calculation at a given basis set was preceded by a full geometry optimization utilizing the identical basis set. The frequencies of the Ag−Py model were calculated with the HF and MP2 methods, and those of the $(Ag-Py)^+$ model, with the HF, MP2, and B3LYP methods. Calculations with the $(Ag_4-Py)^+$ models were done only with the HF method. The Ag_4^+ cluster was optimized first, followed by an optimization of just the pyridine geometrical parameters.

Results

Empirical Normal Mode Calculations. To the best of our knowledge, Suzuki and Orville-Thomas[41] were the first to perform vibrational frequency shift calculations comparing a molecule in the gas phase and when it is bound to a metal ion. In their work, these authors incorporated a metal ion−nitrogen stretching force constant, K(M−N), into the Urey−Bradley force field that they had obtained by fitting the vibrational frequencies in the gas phase spectrum of pyridine. They then adjusted the K(M−N) value to match the M−N stretching frequency, ν(M−N), for a series of pyridine metal ion complexes. The K(M−N) value thus obtained produced a shift to the calculated

frequency of the symmetric ring bending mode, the Wilson mode 6a, that shows up in the gas phase spectrum at 603 cm^{-1}. (Wilson numbers will be used throughout this article to designate the normal modes.) This calculated shift matched the experimental shift observed in the spectra of the pyridine metal ion complexes. The 603 cm^{-1} band actually has the largest frequency shift in most of the pyridine metal complexes studied by Suzuki and Orville-Thomas. Since they were able to reproduce that shift as well as the ν(M−N) mode by just incorporating a K(M−N) into the pyridine force field, those authors concluded that the vibrational interaction between pyridine and a metal ion on coordination was due mostly to kinetic coupling and that the metal−ligand coordination did not produce a significant redistribution of the electron density in the molecule.

The 603 cm^{-1} band is also the band that shifts the most in the SERS spectrum of pyridine obtained on an Ag electrode surface. Thus, in the present investigation, we followed the calculation method of Suzuki and Orville-Thomas and incorporated a silver atom into a Urey−Bradley force field of pyridine in order to reproduce the ν(Ag−N) mode as well as the most significant frequency shifts observed in the SERS spectrum. (By significant frequency shifts we mean those over 10 cm^{-1}.) Those shifts are the ones for the 1581, 1227, 1052, 991, and 603 cm^{-1} bands. These bands correspond to the Wilson modes 8a, 3, 18b, 1, and 6a, respectively. In our case, the addition of a K(Ag−N) force constant and a F(Ag···C_α) constant, for a nonbonded interaction between a silver atom on the surface and the carbon atoms adjacent to the nitrogen, does not reproduce all of the main frequency shifts. These force constants only yielded significant shifts to the 1581, 991, and 603 cm^{-1} bands. This fact suggested, in contrast to what Suzuki and Orville-Thomas observed for the pyridine−metal ion complexes, that the interaction between pyridine and the Ag electrode surface involved some charge density redistribution. Ab initio calculations then provide us a way to determine how the electron density changed, in a relative sense, through the various relations between bond length, bond order, and force constant.[45−47] Vivoni et al.[35] had used this method of adjusting the force constants of 6-mercaptopurine when determining its orientation on a roughened Ag electrode surface.

In the UBFF calculation, a K(Ag−N) value of 1.10 mdyn/Å produced a proper shift of 20 cm^{-1} to the totally symmetric ring breathing mode (1) at 991 cm^{-1} and an overestimated shift of 45 cm^{-1} to the symmetric ring bending mode (6a) at 603 cm^{-1}. Yet, it calculated the ν(Ag−N) mode at only 183 cm^{-1}, way short of the experimental value of 239 cm^{-1}. Increasing the K(Ag−N) such as to match the ν(Ag−N) frequency would have grossly overestimated both 1 and 6a modes. By keeping the 1.10 mdyn/Å value for K(Ag−N) and adjusting the F(Ag···C_α) interaction between the Ag atom and the adjacent carbon atoms to 0.40 mdyn/Å, we obtained a ν(Ag−N) frequency of 239 cm^{-1}. The F(Ag···C_α) force constant did not affect mode 1, but it further increased the shift of mode 6a to 54 cm^{-1}. This overestimation along with the fact that the calculation underestimated the other significant shifts in the SERS spectrum meant that the electron density redistributed around the molecule as it bonded to the surface. To find out how the electron density redistributed, we turned to the ab initio calculations.

The geometry optimization of pyridine compared to a $(Ag-Py)^+$ model with the HF/3-21G method revealed that the N1−C2 bonds lengthened, that the C2−C3 bonds shortened, and that the C3−C4 bonds remained the same when a Ag atom was attached to the nitrogen. Table 2 shows the differences in the bond lengths of the three ring bonds between the free pyridine and the $(Ag-Py)^+$ calculation. A lengthening of a bond means that the bond loses electron density and becomes weaker. Conversely, the shortening of the bond length means that the bond gains electron density and becomes stronger. Moreover, Majoube[48] showed that the magnitude of the bending force constants is inversely proportional to the distances between the corner atoms. The changes in bond length obtained from the ab initio calculation thus justified a decrease in the CNC bending. This force constant contributes significantly to the symmetric ring bending mode 6a, and decreasing it by 0.18 mdyn/Å reduced the error in the calculated shift of that band. Similarly, by increasing the K(C2C3) force constants by 0.20 mdyn /Å and decreasing the K(N1C2) by 0.10 mdyn/Å, the shifts to the 1581, 1227, and 1052 cm^{-1} bands approached more closely the experimental shifts. The frequency shifts that resulted from these calculations are shown in Table 3, and the final force constants, in Table 1.

TABLE 2: Bond Lengths, in Å, of the Ring Bonds of Pyridine and the $(Ag-Py)^+$ Model Calculated with the HF/3-21G Method

	bond length	
bond	pyridine	$(Ag-pyridine)^+$
N1−C2	1.331	1.340
C2−C3	1.383	1.377
C3−C4	1.384	1.384

TABLE 3: Gas Phase Frequency Shifts between the Gas Phase and SERS Spectra of the In-Plane Vibrations of Pyridine Calculated with a Urey−Bradley Force Field

Wilson no.	sym	obsd freq	obsd shift	calcd shift	assignment
8a	a1	1581	15	16	ring stretch
8b	b2	1574	−2	2	ring stretch
19a	a1	1483	−1	1	C−H deformation
19b	b2	1437	7	8	C−H deformation
14	b2	1355		3	C−H deformation
3	b2	1227	11	7	C−H deformation
9a	a1	1217	1	2	ring stretch
15	b2	1146	7	6	ring stretch
18a	a1	1069	−1	−2	C−H deformation
18b	b2	1052	16	9	C−H deformation
12	a1	1030	6	1	trigonal ring breathing
1	a1	991	18	17	totally symmetric ring breathing
6b	b2	654	−3	3	ring deformation
6a	a1	603	24	37	ring deformation

All values in cm^{-1}. Observed frequencies obtained from ref 19 and 43.

Ab Initio Molecular Orbital Calculations. The results of the UBFF calculation just described are consistent with pyridine binding to an adatom on the metal surface by forming a σ-bond through lone pair electrons on the nitrogen. But before performing further ab initio calculations for pyridine, we carried out preliminary calculations with benzene and Ag−benzene models, $(Ag-Bz)^0$ and $(Ag-Bz)^+$, using the UHF/3-21G method to see if those calculations reproduced the vibrational frequency shifts observed in the SERS spectrum. A comparison between the liquid and the SERS spectra of benzene (Table 4) shows the ring stretching modes are shifted down in the SERS spectrum from their positions in the liquid spectrum.[49] Gao and Weaver[50] obtained a SERS spectrum of benzene on a Au electrode that also showed downshifts of the ring stretching modes. These authors attributed the downshifts to the back-donation of electron density from the surface to the π^* antibonding orbitals of benzene as the molecule binds flat on the surface. The comparison between the solution and SERS spectra of benzene

TABLE 4: Frequency Shifts between the Liquid and SERS Spectra of Benzene and between the Gas Phase and SERS Spectra of Pyridine Calculated with Neutral and +1 Charged Models Using the UHF/3-21G Method

	benzene				pyridine				
Wilson no.	obsd freq	obsd shift	$(Ag-Bz)^0$ calcd shift	$(Ag-Bz)^{+1}$ calcd shift	obsd freq	obsd shift	$(Ag-Py)^0$ calcd shift	$(Ag-Py)^{+1}$ calcd shift	assignment
in-plane									
8a	1596	−9	−8	−30	1581	15	10	16	ring stretch
8b	1596	−9			1574	−2	−1	−5	ring stretch
19a	1479	−6	−4	−16	1483	−1	3	9	C−H deformation
19b	1479	−6			1437	7	3	5	C−H deformation
3	1346		−1	−8	1355		0	7	C−H deformation
14	1309	2	3	2	1227	11	3	7	C−H deformation
9a	1178	−1	0	−5	1217	1	0	8	ring stretch
9b	1178	−1							ring stretch
15	1149	0	6	−12	1146	7	12	36	
18a	1036	−4	−4	−18	1069	−1	−1	−2	C−H deformation
18b	1036	−4			1052	16	3	0	C−H deformation
12	1008		−2	−13	1030	6	8	21	trigonal ring breathing
1	992	−10	−6	−22	991	18	7	12	totally symmetric ring breathing
6b	606	−1	−3	−9	654	−3	−3	−6	ring deformation
6a	606	−1			603	24	15	32	ring deformation
out-of-plane									
5	989		−8	−8	1007	2	9	21	C−H twist
17a	966		0	11	980		8	6	C−H twist
17b	966				941	2	12	16	C−H twist
10a	849	15	8	33	884	−3	2	1	C−H twist
10b	849	15				7	7	13	C−H twist
4	703		−13	−32	747	2	−3	−6	ring twist
11	670	27	14	49	703	8	3	2	C−H twist
16a	404	−7	−11	−1	406	7	−1	−2	ring twist
16b	404	−7			380				ring twist

(Observed frequencies of benzene are from ref 49 and of pyridine from ref 43.)

also shows that the hydrogen out-of-plane vibrations are shifted up in the SERS spectrum. The results of the UHF/3-21G calculations of the free benzene molecule and the $(Ag-benzene)^+$ model are shown in Table 4. In the latter case, the Ag atom is placed in the center of the aromatic ring and 2 Å away from it. From this table, we can see that the calculations with the $(Ag-benzene)^+$ model yielded, for the most part, frequency shifts that were analogous to the ones observed in the SERS spectrum, that is, in the same direction but not necessarily by the same amount.

In the SERS spectrum of pyridine, ring stretching modes shift upward and the out-of-plane modes remain practically unchanged (Table 4). This fact by itself already suggests that pyridine has a different orientation at the surface active site than benzene. As with the benzene calculations, the initial HF/3-21G calculations with a free pyridine molecule and a $(Ag-Py)^+$ model yielded frequency shifts that were analogous to the ones observed in the SERS spectrum. The results of these calculations are shown in Table 4 along with those of benzene. The fact that the ab initio calculations at the 3-21G level yielded frequency shifts analogous to the experimental shifts for both benzene and pyridine indicates that the single adatom model is an adequate approximation for the molecule−Ag surface interaction. In fact, the semiempirical calculations[9] of a pyridine−Ag_n clusters model (n = 10, 13, 14, 15) show that 80% of the bonding is localized between the pyridine N atom and its nearest neighbor Ag atom. We thus proceeded further with higher level ab initio calculations and turn first to free molecule calculations.

Free Molecule Calculation. Yang and Schatz[37] have made scaled Hartree−Fock HF/6-311++G frequency calculations for pyridine in a vacuum. We repeated these calculations with other basis sets and MP2 and DTF calculations for comparison to results when Ag is included in the chemical model of the scattering species. Our model of pyridine in a vacuum was initially constructed with Hartee-Fock, MP2, and B3LYP methods, and frequencies were subsequently obtained for the 3-21G, 6-31G, 6-31G*, 6-31G**, and LanL2DZ basis sets. These calculations followed a full geometry optimization with each basis set. The calculated frequencies were scaled at the HF level by dividing the experimental value for the totally symmetric ring-breathing (mode 1) by the calculated value. Mode 1 is the most intense peak on the pyridine spectrum.

Table 5 shows a comparison of the scaled frequencies of the in-plane normal modes with the experimental frequencies of pyridine. The average relative error does not show much difference between scaled 6-31G, 6-31G*, 6-31G**, and 6-311++G at the Hartree−Fock level. Scaled results with the LanL2DZ basis set at the HF level seem to have slightly more error. However, of these basis sets, the LanL2DZ has the advantage, for our purposes, that it has been extended to include the silver atom. Of the other basis sets, only 3-21G includes Ag. Thus, with Ag incorporated in the chemical model, we used either a mixed basis set with 3-21G for Ag and one of the larger basis sets for pyridine or the LanL2DZ basis set for both with either the HF, MP2, or B3LYP calculational methods.

The unscaled results of the MP2 and B3LYP calculations are also shown in Table 5. It is interesting to point out that the frequencies in the MP2 calculations are not all linearly overestimated, as they are in the HF calculations. The low end frequencies tend to be very close to the experimental ones or slightly underestimated. On the other hand, the upper range frequencies are all overestimated; but even those were not overestimated in a linear fashion, as was the case for the HF calculation. On the whole, the MP2 calculation produced a 4.0% average error from the experimental values with the 6-31G** basis set and only a 1.4% average error with the LanL2DZ basis set. In comparison, the unscaled B3LYP calculation with the LanL2DZ basis set had a slightly larger average of 2.5% error

TABLE 5: Comparison of Observed Gas Phase Frequencies of Pyridine (Ref 43) against the Scaled Calculated Frequencies in Wavenumbers

			calcd freq								
Wilson no.	obsd freq	method: basis set: scale factor:	HF 3-21G 0.9151	HF 6-31G 0.9056	HF 6-31G* 0.9059	HF 6-31G** 0.9067	HF[a] 6-311++G 0.90	HF Lan L2 DZ 0.9227	MP2 6-31G**	MP2 LanL2DZ	B3LYP LanL2DZ
8a	1581		1600	1617	1631	1631	1583	1633	1662	1573	1613
8b	1574		1594	1609	1622	1622	1577	1628	1652	1567	1616
19a	1483		1513	1503	1505	1501	1475	1510	1537	1479	1499
19b	1437		1470	1462	1457	1453	1435	1471	1501	1448	1469
14	1355		1398	1379	1368	1362	1356	1392	1414	1382	1394
3	1227		1214	1210	1191	1190	1185	1149	1401	1272	1307
9a	1217		1238	1227	1221	1220	1205	1242	1264	1232	1249
15	1146		1090	1135	1074	1073	1101	1070	1199	1187	1195
18a	1069		1097	1080	1072	1070	1060	1086	1110	1077	1090
18b	1052		1060	1064	1054	1051	1040	1071	1098	1057	1077
12	1030		1041	1031	1017	1018	1038	1037	1056	1028	1042
1	991		991	991	991	991	1013	991	1014	947	989
6b	654		685	668	652	653	658	669	666	656	669
6a	603		630	616	597	598	607	617	609	607	616
av rel error[b]			2.2	1.4	1.6	1.5	1.1	2.6	4.4	1.4	2.4

[a] Results of Yang and Schatz. *J. Chem Phys.* **1992**, *97*, 3831. [b] average relative error = {Σ[abs(calcd − obsd)/obsd] × 100%}/14.

TABLE 6: Comparison of Observed and Calculated SERS Vibrational Frequency Shifts in Wavenumbers[a]

			calcd shift								
		model:	$(Ag-Py)^0$			$(Ag-Py)^+$					$(Ag_4-Py)^+$
gas phase obsd freq	obsd shift	method: basis set:	HF 3-21G//6-31G**	HF LanL2DZ	MP2 LanL2DZ	HF 3-21G//6-31G**	HF LanL2DZ	MP2 3-21G//6-31G**	MP2 LanL2DZ	B3LYP LanL2DZ	HF LanL2DZ
1581	15		8	6	12	12	15	22	32	28	17
1574	−2		0	0	−2	−8	−7	−2	4	−6	−5
1483	−1		1	4	0	4	11	6	17	11	10
1437	7		3	4	13	6	8	16	18	15	7
1227	11		3	1	1	6	19	7	31	14	6
1217	1		−5	2	5	1	11	5	17	8	10
1146	7		6	6	6	23	16	12	19	18	14
1069	−1		−1	−1		−1	−4	1	−6	−2	−1
1052	16		10	5	10	18	5	16	15	19	14
1030	6		−3	6	9	12	23	4	31	16	5
991	18		9	5	20	15	12	30	34	29	12
654	−3		−3	−2	−1	−6	−5	−5	−2	−7	−3
603	24		12	8	19	28	31	31	39	39	26

[a] Observed SERS shifts were calculated by subtracting observed normal Raman frequencies (ref 43) from observed SERS frequencies (ref 19). Calculated shifts were obtained by subtracting unscaled calculated frequencies of the adatom models from unscaled pyridine values (Table 5).

but was found to be computationally more efficient than the MP2 calculation.

Adatom Complex Calculation. After calculating the free molecule normal modes, we built the initial Ag−Py model by attaching an Ag atom edge-on to the nitrogen on the pyridine. This model simulates an edge-on interaction of the molecule with an on-top adatom on the Ag surface. We performed the calculations with the HF, MP2, and B3LYP methods using two types of basis sets: the LanL2DZ basis set or a split basis set composed of 3-21G for the silver atom and 6-31G** for the pyridine molecule, respectively. We will henceforth refer to this set as 3-21G//6-31G**. We performed B3LYP calculations with just the LanL2DZ basis set. The results of these calculations are given in Table 6 in terms of a comparison of the observed shift in wavenumbers between the normal Raman scattering spectrum in the gas phase and the SERS spectrum and the calculated shifts between the three chemical models involving pyridine interacting with an Ag adatom in the on-top (σ-bonded) structure and pyridine in a vacuum. Table 6 shows the extent to which for the strong SERS bands the calculated shifts with the Ag adatom models correspond to the experimentally observed shifts.

First observe the extent to which the Ag−pyridine models reproduce the ν(Ag−N) stretch which appears at ∼239 cm^{-1} in the SERS spectrum of pyridine. Table 7 shows the Ag−N bond distance and Ag−N stretching vibration for the three models. The neutral Ag−pyridine edge-on model, immensely

TABLE 7: Calculated Ag−N Bond Length and Ag−N Stretch Observed at 239 cm^{-1} on the Pyridine SERS Spectrum, with the Various ab Initio Methods

species	method basis set	ν(Ag−N) freq (cm^{-1})	Ag−N bond length (Å)
$(Ag-Py)^0$	HF 3-21G//6−31**	96	2.58
	HF LanL2DZ	64	2.69
	MP2 LanL2DZ	119	2.45
$(Ag-Py)^+$	HF 3-21G//6-31G**	170	2.33
	HF LanL2DZ	181	2.29
	MP2 3-21G//6-31G**	177	2.29
	MP2 LanL2DZ	197	2.24
	B3LYP LanL2DZ	198	2.17
$(Ag_4-Py)^+$	HF LanL2DZ	252	2.33

TABLE 8: Voltage Dependence, versus SCE, of the Vibrational Frequencies in the SERS Spectrum of Pyridine Obtained on a Ag Electrode

Wilson no.	−0.2 V	−0.4 V	−0.6 V	−0.8 V
8a	1624	1626	1630	1624
8b	1594	1594	1592	1592
9a	1216	1216	1214	1214
18a	1066	1066	1064	1066
12	1036	1036	1036	1034
1	1006	1006	1006	1006
6b	648	648	648	648
6a	626	624	624	622
16a	414	414	412	410
ν(Ag−N)	232	228	218	206

underestimated the 239 cm^{-1} by 119−143 cm^{-1}. An Onsager SCRF calculation for solvation caused a slight positive shift, but not enough to be of sufficient effect. The calculation of the atomic charges suggested a possible explanation to the underestimated ν(Ag−N) stretch, since they showed that both the Ag and N atoms were negatively charged, thus resulting in a weak bond. The calculation was subsequently repeated with a positive charge delocalized over the entire Ag−Py model. This calculation improved the calculated value of the 239 cm^{-1} frequency, and for the MP2 and B3LYP methods with the LanL2DZ basis set, the unscaled value was only 40 cm^{-1} on the low side. To improve the value of the ν(Ag−N) stretch, calculations were carried out with a molecular model that represented the surface active site as a pyramidal Ag_4^+ cluster, as proposed by Roy and Furtak. These calculations were made with the HF method using the LanL2DZ basis set. In this manner, the 239 cm^{-1} frequency was calculated at 252 cm^{-1}. Scaling this value by the 0.9227 factor obtained from the gas-phase calculation for the LanL2DZ basis set yields a 233 cm^{-1} calculated frequency. This value is quite close to the experimental value. Table 7 gives all of the calculated values for the ν(Ag−N) stretching mode.

In an electrochemical environment, the ν(Ag−N) stretching mode frequency shifts to lower values as the potential at a Ag electrode surface becomes more negative and also shifts with counteranion of the electrolyte. In recent experiments with pyridine in an electrochemical environment, we find, on an activated Ag electrode at −0.2 V versus SCE, the ν(Ag−N) band at 240, 232, and 226 cm^{-1} in 0.1 M K_2SO_4, KCl, and KF, respectively. Thus, the above calculated value is quite close to all of these experimental values. The experimental setup for these measurements is the same as that we used in our previous measurements[51] except that in the present case we use an in situ oxidation reduction cycle. Table 8 shows several assigned bands from these spectra as a function of electrode potential for 0.1 M KCl. We should mention that the spectra obtained in our laboratory are almost identical to spectra recently reported for the same system by Li et al.[52] at −0.2, −0.4, −0.6, and −0.8 V. In both studies, the only band position which shifts with electrode potential is the ν(Ag−N) stretching mode. We note that the lowering of the frequency of this band as the potential becomes more negative implies that the Ag−N bond becomes weaker at the more negative potential. We also note that we find similar results for the K_2SO_4 and KF electrolyte systems; that is, the ν(Ag−N) stretching mode shifts down with a negative shift in voltage but the internal modes do not shift.

We were the first to point out that the so-called surface Ag-molecule band shifts with electrode potential in SERS spectra,[53] and we attributed this shift to a vibrational Stark effect. A chemical bonding interpretation of this effect was subsequently given by Anderson et al.[54] for cyanide on a Ag electrode surface. The latter authors made a similar bonding assumption to the one we are making herein, namely that cyanide is bonded to one Ag atom of a Ag cluster, Ag_4−CN. They reasoned that a change in electrode potential is equivalent to a change in the ionization potential of Ag and, using semiempirical calculations, found that a positive shift in potential causes more charge donation from a cyanide to Ag in a σ_p orbital with antibonding character, which increases both ν(CN) and ν(Ag−C). The same bonding geometry was used by Lin et al.[55] using the self-consistent-charge variational Xα(SCC-DV-Xα) calculation method. These workers also found that the dominant charge donation is σ donation from the cyanide to the on-top Ag atom and that a positive charge on the Ag_4 cluster increased the charge donation.[55] A similar situation exits for pyridine on Ag, since the surface bond is formed by charge donation from the nitrogen to a Ag atom of the cluster.

We can interpret differences in the frequency shifts in the SERS spectrum of pyridine obtained at various potentials as being due to variation in the strength of the Ag−N bond. This should not come as a surprise, since, as Rodriguez[9,11] demonstrated for cluster models of Ag surfaces, the bond between the pyridine and a metal surface forms by the donation of charge density from the nitrogen to a Ag atom on the surface and a more negative potential on the surface hinders the charge donation, thus inducing a weakening of the bond.

While the Ag_4^+ cluster model of the surface best reproduced the ν(Ag−N) frequency, it is still important to consider the effect of pyridine binding to Ag on the other vibrations. From Table 6 we see that the calculations that best reproduce the experimental shifts were those at the MP2/3-21G//6-31G**, MP2/Lan2DZ, and B3LYP/LanL2DZ levels for the $(Ag-Py)^+$ model and HF/LanL2DZ for the $(Ag_4-Py)^+$ model. The empirical normal mode calculations compared to the HF/3-21G calculations showed that formation of the coordinating bond to the nitrogen of pyridine in turn influenced the SERS spectrum through the redistribution of charge in the ring. We examine this influence by employing natural bond orbital, NBO, calculations implemented in Gaussian 98 using the $NBO BNDIDX NLMO $END keywords. The calculations were done at the restricted B3LYP/LanL2DZ level for pyridine and $(Ag-Py)^+$ model systems. Below are the Wiberg bond order index (the sum of squares of the off diagonal matrix elements) for the N1−C2 (C6−N1), C2−C3 (C5−C6), and C3−C4 (C4−C5) bonds obtained from the calculation.

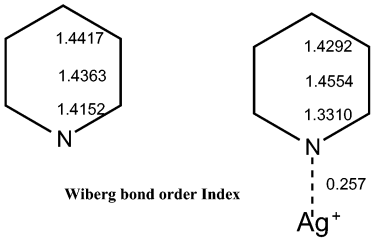

We observe that upon interaction with Ag^+ the C2−C3 (C5−C6)) bond order in the pyridine ring increases and the other two decrease. The Wiberg bond order found for N−Ag is 0.257, which is consistent with a weak covalent chemical bonding interaction between Ag and the ring nitrogen, and the natural population analysis, NPA, gives a charge of +0.87 on Ag and −0.68 on N, showing that most of the positive charge is on the Ag (Mulliken populations put a much lower charge on both, +0.67 on Ag and −0.29 on N). Another measure of the bonding is the natural localized molecular orbital, NLMO, bond order,

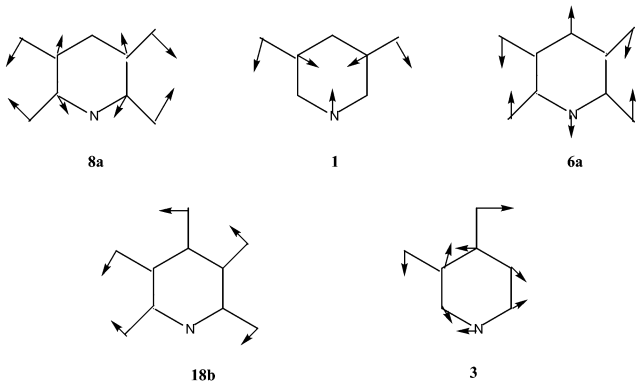

Figure 1. Normal modes (in Wilson numbers) of the frequencies that shift by more than 10 cm^{-1} in the SERS spectrum of pyridine. The modes were taken from the displacement vectors found by the B3LYP/LanL2DZ method.

which gives a bond order of 0.136 with a hybrid overlap of 0.437 between the N−Ag atoms with an atomic hybrid donation of 6.802% from the nitrogen lone pair to Ag orbitals. The percent mixing with the Ag orbitals is 5s (95.85%), 5p (1.65%), and 4d (2.50%). Thus, the bonding of pyridine to an on-top positively charged Ag adatom site on the silver surface involves donation of a small amount of charge from the N lone pair mostly to the vacant 5s Ag orbital. Second-order perturbation theory energy analysis of the Fock matrix in the NBO basis shows that the largest stabilization energy $E(2) = 28.7$ kJ/mol on Ag comes from delocalization of the lone pair NLMO on nitrogen to the NLMO lowest vacant Ag orbital, Ag(5s). Thus, the weakening of the Ag−N bond as the potential is moved negative is consistent with a decrease in this stabilization energy. The second-order perturbation analysis also shows a small amount of back-donation from Ag(4d) orbitals to N−C antibonding NLMOs with a total stabilization energy from this process of 2.6 kJ/mol.

Discussion

On examining the frequency shifts in the SERS spectrum, we observe that the normal modes that shift the most are the symmetric ring breathing (mode 1), the ring bending (mode 6a), and the C−H deformation (mode 18b). Modes 1 and 6a involve the nitrogen vibration and have a_1 symmetry, as seen in Figure 1. Because of their symmetry, the vibration of the nitrogen in normal modes 1 and 6a is along the molecular axis and, thus, in the direction of the Ag atom. The results of the UBFF calculations are therefore as expected, since those normal modes are the ones most affected by the K(Ag−N) force constant. The next largest shifts in the SERS spectrum are from the ring stretching (modes 18b and 8a) and also contain contributions from C−H in-plane bending. Normal mode 8a has its largest contribution from the C2−C3 stretching motion. As with modes 1 and 6a, the 8a normal mode has a_1 symmetry and the carbon atoms α to the nitrogen vibrate roughly in the direction of the Ag atom. While the F(Ag···C_α) did not reproduce the complete shift of this mode, it did reproduce two-thirds of it. The rest of the shift was accounted for by the increase of the K(C2C3) force constant. The other two bands that show significant shifts in the SERS spectrum are the gas phase ones at 1227 and the 1052 cm^{-1} (Figure 1), corresponding to the Wilson modes 3 and 18b, respectively. Both of these normal modes have b_2 symmetry, and mode 3 has a large contribution from the C2−C3 stretch. Because these modes are antisymmetric, the vibrations of the α carbons are perpendicular to the direction of the K(Ag−N) and the F(Ag···C_α) force constants and thus not affected by them. The shifts to these normal modes are instead due to the electron density redistribution within the ring. This fact is also clear from the ab initio calculations on comparing pyridine by itself with Ag adatom−pyridine models using the MP2 and B3LYP calculational methods. The calculations (Table 6) show substantial frequency upshifts for normal modes 1, 6a, 18b, 3, and 8a which contain a contribution from C2−C3 (C5−C6) motion. This redistribution of the ring electronic structure leads to an electronic structure with more contribution from a quinoid resonance form, as shown by the Wiberg bond order index.

The observations just described are consistent with an edge-on form of attachment of pyridine to the electrode surface. They also provide a justification for including a F(Ag···C_α) force constant in the calculation even though Suzuki and Orville-Thomas did not use it in their pyridine metal ion-complex calculations. Further justification for using the F(Ag···C_α) comes from the work of Rodriguez.[9,11] From INDO/S calculations, this author found that the nitrogen provides approximately 80% of the total charge donated by pyridine and the rest of the charge is donated through the C_α and the hydrogen atoms bonded to the C_α, about 20% when pyridine is absorbed on cluster models of Ag(100) and Ag(111) surfaces. Our NLMO analysis for $(Ag-Py)^+$ did not show significant charge donation from C_α orbitals to Ag orbitals. Both our calculations and those of Rodriguez indicate that the Ag −N bond is mostly between the N atom and the nearest-neighbor Ag atom. Moreover, Rodriguez[11] also found that, in the case of a Cu(111) surface, the Cu atom bonded to pyridine donates a small amount of charge density into the C−N antibonding orbital (π-back-bonding). The second-order perturbation analysis for charge donation from filled to unfilled orbitals in the NBO basis showed a delocalization energy of 28.7 kJ/mol for the lone pair orbital on N to the vacant 5s orbital on Ag in comparison with 2.6 kJ/mol for donation from filled Ag(4d) orbitals to C−N vacant π-antibonding orbitals. This back-bonding should strengthen the nonbonding Ag···C_α interaction; however, its main effect would be to weaken the bond between nitrogen and the adjacent carbons in pyridine.

The frequency shifts in the SERS spectrum of pyridine are also observed in comparing pyridine solution and metal ion-complex spectra. From Table 9 we notice the same frequencies shift upward in all of these spectra. The tendency is an increasing frequency shift on going from the solution spectrum to the SERS spectrum and to the metal ion-complex spectrum. From this tendency one could surmise that the frequency shifts are directly related to the strength of the bonding at the nitrogen position. Frequency shifts in the case of solution spectra of pyridine were previously noted by Takahasi et al.[56] and attributed to the formation of a hydrogen bond between the nitrogen and a water molecule. Because of the weakness of the hydrogen bond, the bond that forms between pyridine and a water molecule is expected to be the weakest of the three bonds that the nitrogen can form. The frequency shifts of the pyridine Ag ion-complex are due to the σ-bond between the nitrogen on the pyridine and an Ag^+ ion. This bond is expected to be the strongest in the three types of Raman spectra because it forms with the full positive ion as with all metal ion-complexes. This view is supported by the fact that the ν(Ag−N) band in the $(Ag-Py_2)^+$ complex is 5 cm^{-1} higher than that in the SERS spectrum of pyridine. The ab initio calculations also yield a higher ν(Ag−N) mode with the $(Ag-Py)^+$ model than with the $(Ag-Py)^0$ model. This should be as expected, since the +1 charge in the $(Ag-Py)^+$ model is mostly on the Ag and should enhance the

TABLE 9: Observed Frequency Shifts (in cm^{-1}) in the Solution, SERS, and Ag(Py)$_2^+$ Complex Spectra of Pyridine

		observed frequency shifts		
Wilson no.	gas phase[a]	solution[b]	SERS[b]	Ag(Py)$_2^+$ [b]
in-plane				
8a	1581	12	15	23
8b	1574	2	−2	−2
19a	1483	4	−1	6
19b	1437	7	7	
14	1355			
3	1227	5	11	
9a	1217	3	1	10
15	1146	7	7	10
18a	1069	2	−1	2
18b	1052		16	
12	1030	6	6	9
1	991	11	18	21
6b	654	0	−3	−7
6a	603	15	24	30
out-of-plane				
5	1007	−5	2	
17a	980			
10b	941	7	2	
10a	884	3	−3	
4	747	13	7	9
11	703	5	2	−2
16b	406	5	8	9
16a	380	5	7	

[a] Reference 43. [b] References 19.

charge donation from the nitrogen to the Ag atom. In fact, the calculation with the neutral model yielded negative partial charges on both the Ag and the N atoms, which produce a weaker bond.

From Tables 4 and 6 one also sees that, in general, the ab initio methods predicted shifts in the same direction as those observed experimentally. Moreover, the neutral model underestimated many of the shifts while the +1 model overestimated many of them. Those results suggest that the actual charge on the adatom in the surface active site is somewhere between 0 and +1. This inference is supported by the fact that the $(Ag_4-Py)^+$ model was the one that best fitted the observed frequency of the external mode and the frequency shifts of the internal modes. In this model, the positive charge is distributed mostly throughout the four Ag atoms and, therefore, the Ag atom bonded to the nitrogen of pyridine has a partial charge.

Only the shift of the 19a band to 1483 cm^{-1} was not adequately reproduced by the ab initio calculations. This discrepancy is rather small but may be due to a surface property not accounted for by any of the models used in the calculations. Despite this, a good correlation between the calculated and experimental SERS shifts was observed for all other bands.

One final observation about ab initio calculations is the calculated Ag−N bond length (Table 7). Although there is no direct measure of this bond length when pyridine is adsorbed on the electrode surface, that distance is likely to be close to the Ag−N distance of 2.322 Å found from X-ray crystallography for the $Ag(Py)_4^+$ complex ion.[42] Lombardi et al.[13] determined that the lower limit of the Ag−N distance for lutidine is 2.5 Å. However, a more accurate lower limit for pyridine is probably closer to the sum of the covalent radii, 2.2 Å, since the Ag−N bond is not expected to be as strong as a covalent bond. A 2.322 Å Ag−N bond length would also be in accord with the Ag_4^+ cluster model for the surface proposed by Roy and Furtak, since the charged experienced by each pyridine will only be one-fourth of the total single charge. It should be noticed that all of the $(Ag-Py)^+$ calculations with the LanL2DZ basis set yielded Ag−N distances less than those of any of the other calculations. The $(Ag_4-Py)^+$ model had the most reasonable values for both the ν(Ag−N) frequency and the Ag−N distance.

Conclusion

All of the results in this work point toward an edge-on interaction between pyridine and an Ag adatom in the roughened electrode surface. However, the intensity ratio analysis based on surface selection rules[19,24] indicates that the pyridine molecule can lie flat[19] with respect to the Ag surface so that normal modes are enhanced which have polarizibility tensor elements which couple into the tangential component of the electric field of the exciting light. On the other hand, Creighton[19] also found that the vibrational frequency shifts in the SERS spectrum were characteristic of a pyridine metal-complex spectrum where the molecule binds edge-on to the metal atom. He attempted to reconcile both phenomena by proposing the formation of a pyridine complex, $Ag(Py)_2^+$, which might form near the electrode surface and be adsorbed onto the surface during the ORC pretreatment. Since the pyridine molecules are collinear in this complex, they align parallel to the surface when the complex binds to the surface.

We have found that both ex situ and in situ pretreatment give similar SERS spectra, suggesting some kind of a pyridine adatom-complex forms on the surface even after ex situ pretreatment. However, our calculations show that it is not necessary to conclude that a complex forms with two pyridine ligands. A single pyridine molecule bound to a Ag adatom of a Ag cluster is certainly an adequate model. In fact, the pyridine could be σ-bonded to the Ag cluster in an in-plane (flat) or above-plane (vertical) configuration. If the active site on the surface is composed of an adatom sitting on top of three other Ag atoms, as in the Ag_4 pyramidal structure, the whole pyramidal structure could lie on top of another layer of Ag atoms, perhaps the surface layer. This type of arrangement would allow for the formation of a surface site with the adatom on top of the trigonal pyramid. It would also raise the pyridine ligand just enough over the surface so that it did not show the frequency shift patterns observed in benzene that are characteristic of a face-on interaction with a Ag adatom. At the same time, this structure would keep it close enough to the surface so that it could interact with the electromagnetic field on the surface.

This model explains why pyridine is able to change its orientation with respect to surface potential, as we have observed.[27] The pyridine ligand in the adatom complex could go from a linear alignment to an angular alignment, as in the case of the $Ag(Py)_4^+$ ion in the solid state. If it were the case that a $Ag(Py)_2^+$ complex formed on the surface, the two pyridine molecules could not stand up in a completely perpendicular position, as proposed by several authors for various heteroaromatic molecules that bond to the surface through the nitrogen atom. [17,25,38,57,58] For pyridine to stand up completely perpendicular to the surface, either a pyridine ligand loses its coordination to the adatom upon voltage change or the adatom-complex has only one pyridine ligand.

Our models of the SERS chemisorbed complex have been simplified, since if coadsorbed Cl^- and H_2O molecules are nearest-neighbors to chemisorbed pyridine, they might need to be considered in addition to more Ag atoms in the surface metal cluster site in order to reproduce all the properties of the SERS spectrum in ab initio calculations. Both Roy and Furtak[28] and Wantanabe et al.[59] provided experimental evidence for a Ag^+ species as a constituent of the Ag electrode SERS active site.

The Ag_4^+ cluster was proposed by Roy and Furtak[28] as the dominant active site in an electrochemical environment on the basis of the observation of the Ag cluster vibrational modes whose frequencies are near those calculated by a normal-mode analysis. Ag_n^+ clusters produced in the gas phase and mass selected show an odd−even alternation in nuclearity where Ag_3 and Ag_5 are more abundant than Ag_4 and where Ag_6 and Ag_8 are almost absent.[60] On the other hand, if the active site was a Ag_5 cluster, it might be expected to show more low-frequency Raman bands[61] than the three observed at the Ag electrode,[28] especially if its Raman spectrum was surface enhanced. Furthermore, Ag_4^+ formed by photoreduction of Ag(I) and aggregation of the metal Ag atoms in H_2SO_4 has been experimentally observed by ESR,[62] and semiempirical MO calculations show that Ag_4^+ is a stable species with respect to Ag_4.[63] This Ag_4^+ cluster species provides a positively charged metal−molecule chemisorbed system, and our ab initio calculations at the HF level with pyridine binding to this cluster show the upshifts in Raman bands of the internal modes of pyridine found in the electrochemical environment as well as a reasonable value of ν(Ag−N). However, the ab initio calculations with the simple $AgPy^+$ model also reproduce these features almost as well.

Additionally, the fact that the internal modes of pyridine found in the SERS spectra at a Ag electrode do not shift as the voltage is made negative can be explained by the ab initio calculations, since the dominant bonding interaction in this surface complex is the coupling between the lone pair nitrogen electrons and a vacant 5s orbital on the Ag with little contribution from ring pyridine orbitals. Since the bond between the pyridine and the Ag surface forms by the donation of charge density from the nitrogen to the Ag adatom of the cluster, a more negative potential on the surface should hinder the charge donation by shifting the bonding orbitals in such a way as to reduce overlap, thus inducing a weakening of the bond. The experimental SERS results showing a decrease in ν(Ag−N) as the potential is made more negative are consistent with this weakening of the Ag−N bond.

While we originally attributed the lowering of the external mode with voltage to a vibrational Stark effect,[53] which is consistent with the effect of electric field on the molecular dipole moment function at the metal−molecule interface,[64] the alternate approach of a chemical bonding explanation based on ab initio calculations may be more productive. In principle, such a treatment also has the possibility of calculating enhancement factors for our charge transfer theory[65] and other chemical theories[66] of the SERS enhancement where chemical bonding between the molecule and the surface is required. The main problem is how to quantitatively model the effect of voltage at the molecular level in ab initio calculations. In most cases the charge on the metal cluster has been used to model the effect of electrode potential on bonding and vibrational frequencies, as was done in a relatively recent study of the effect of potential on the SERS spectra of SCN^- adsorbed on an Ag electrode.[67] Here the cluster species, Ag_4SCN^-, was used with the variational Xα calculation method, as in ref 55, to calculate the effect of electrode potential (charge on Ag_4SCN^- species) on bonding and (by implication) on the frequency behavior of the ν(CN) stretching vibration of SCN^-. On the other hand, to make very accurate calculations of SERS band positions and the effect of electrode potential on these bands, a model with a much larger number of metal atoms may be necessary. In such a complete model, the active site would have the SERS active molecule and counterions binding to a small metal cluster which itself is bonded to a larger metal cluster representing the roughened metal surface particle. However, the present small cluster model with calculations at either the HF or B3LYP level and a medium sized basis set like LanL2DZ can reproduce SERS band positions for pyridine at a Ag electrode surface.

Acknowledgment. The authors thank Asta Gindulyte and Michael Levine for carrying out the initial Hartree−Fock calculations. J.R.L. and R.L.B. are indebted to the PSC-BHE Research Award Program of the City University of New York, J.R.L. is indebted to the National Science Foundation (CHE-0091362), and R.L.B. is indebted to the National Institutes of Health (SCORE Grant GM08168) for financial support.

References and Notes

(1) Fleishman, M.; Hendra, P. J.; McQuillan, A. J. *Chem. Phys. Lett.* **1974**, *26*, 163.
(2) (a) Kneipp, K.; Kneipp, H.; Itzkan, I.; Dasari, R. R.; Feld, M. S. *Chem. Rev.* **1999**, *99*, 2957−2956. (b) Campion, A.; Kambhampati, P. *Chem. Soc. Rev.* **1998**, *27*, 241−250.
(3) Doering, W. H.; Nie, S. *J. Phys Chem. B* **2020**, *106*, 311−317.
(4) Kennedy, B. J.; Spaeth, S.; Dikey, M.; Carron, K. T. *J. Phys Chem. B* **1999**, *103*, 3640−3646.
(5) Hill, W.; Fallourd, V.; Klocjow, D. *J. Phys Chem. B* **1999**, *103*, 4707−4713.
(6) Cao, Y.-W.; Jin, R.; Mirkin, C. A. *Science* **2002**, *297*, 1536−1540.
(7) Birke, R. L.; Lombardi, J. R. In *Spectroelectrochemistry: theory and practice*; Gale, R. J., Ed.; Plenum Publishing Corporation: New York, 1988; pp 263−347.
(8) Bagus, P. S.; Pacchioni, G.; Philpott, M. R. *J. Chem. Phys.* **1989**, *90*, 4287−4295.
(9) Rodrigues, J. A. *Surf. Sci.* **1990**, *226*, 101−118.
(10) Bagus, P. S.; Herman, K.; Bauschlicher, C. W., Jr. *J. Chem. Phys.* **1984**, *81*, 1966−1974.
(11) Rodrigues, J. A. *Surf. Sci.* **1992**, *273*, 385−404.
(12) Kasser, W.; Kettler, U.; Bechthold, P. S. *Chem. Rev. Lett.* **1982**, *86*, 223−227.
(13) Lombardi, J. R.; Shields Knight, E. A.; Birke, R. L. *Chem. Phys. Lett.* **1981**, *79*, 214−218.
(14) Creighton, J. A.; Albrecht, M. G.; Hester, R. E.; Matthew, J. A. D. *Chem. Phys. Lett.* **1978**, *55*, 55−58.
(15) van Duyne, R. P. In *Chemical and biochemical application of lasers*; Moore, C. B., Ed.; Academic Press: New York, 1979; Vol. 4, Chapter 5, pp 101−185.
(16) Evans, J. F.; Albrecht, M. G.; Ullevig, D. M.; Hexter, R. E. *J. Electroanal. Chem.* **1980**, *106*, 209−234.
(17) Neto, N.; Muniz-Miranda, M.; Sbrana, G. *J. Phys. Chem.* **1996**, *100*, 9911−9917.
(18) Muniz-Miranda, M.; Neto, N.; Sbrana, G. *J. Phys. Chem.* **1988**, *92*, 954−959.
(19) Creighton, J. A. *Surf. Sci.* **1983**, *124*, 209−219.
(20) Netzer, F. P.; Bertel, E.; Matthew, J. A. D. *Surf. Sci.* **1980**, *92*, 43−52.
(21) Surman, M.; Bare, S. R.; Hoffman, P.; King, D. A. *Surf. Sci.* **1987**, *179*, 243−253.
(22) Dudde, R.; Koch, E. E.; Ueno, N.; Engelhardt, R. *Surf. Sci.* **1986**, *178*, 646−656.
(23) Bridge, M. E.; Connolly, M.; Lloyd, D. R.; Somers, J.; Jakob, P.; Menzel, D. *Spectrochim. Acta A* **1987**, *43*, 1473−1478.
(24) Moskovits, M.; Suh, J. S. *J. Chem. Phys.* **1984**, *88*, 5526.
(25) Golab, J. T.; Sprague, J. R.; Carron, K. T.; Schatz, G. C.; Van Duyne, R. P. *J. Chem. Phys.* **1988**, *12*, 7942−7951.
(26) Billman, J.; Kovacs, G.; Otto, A. *Surf. Sci.* **1980**, *92*, 153−173.
(27) Bunding, K. A.; Birke, R. L.; Lombardi, J. R. *Chem. Phys.* **1980**, *54*, 115−121.
(28) Roy, D.; Furtak, T. E. *Chem. Phys. Lett.* **1986**, *124*, 299−303. (b) Roy, D.; Furtak, T. E. *Phys. Rev. B* **1986**, *344*, 5111−5117.
(29) Corni, S.; Thomasi, J. *J. Chem. Phys.* **2002**, *116*, 1156−1164.
(30) Cornis S.; Thomasi, J. *J. Chem. Phys.* **2001**, *114*, 3739−3751.
(31) Corni, S.; Thomasi, J. *Chem. Phys. Lett.* **2001**, *342*, 135−140.
(32) Kwon, Y. J.; Son, D. H.; Ahn, S. J.; Kim, M. S.; Kim, K. *J. Phys. Chem.* **1994**, *98*, 8481−8487.
(33) Cardini, G.; Muniz-Miranda, M. *J. Phys. Chem.* **2002**, *106*, 6875−6880.
(34) Arenas, J. F.; Soto, J.; López Tocón, I.; Fernández, D. J.; Otero, J. C. *J. Chem. Phys.* **2001**, *116*, 7207−7216.

(35) Vivoni, A.; Chen, S.-P.; Ejeh, D.; Hosten, C. M. *Langmuir* **2000**, *16*, 3310−3316.
(36) Aroca, R. F.; Clavijo, R. E.; Halls, M. D.; Schlegel, H. B. *J. Phys. Chem. A* **2000**, *104*, 9500−9505.
(37) Yang, W. H.; Schatz, G. C. *J. Chem. Phys.* **1992**, *97*, 3831−3845.
(38) Muniz-Miranda, M. *J. Phys. Chem*. **2000**, *104*, 7803−7810.
(39) Barlow, A.; Diem, M. *J. Chem. Educ.* **1991**, *68*, 35−39.
(40) Vivoni, A.; Birke, R.; Lombardi, J. *Spectrochim. Acta A* **2001**, *57*, 535−544.
(41) Suzuki, S.; Orville-Thomas, W. J. *J. Mol. Struct.* **1976**, *37*, 321−327.
(42) Nilsson, K.; Oskarsson, A. *Acta Chem. Scand. A* **1982**, *36*, 605−610.
(43) Stidham, H. D.; DiLella, D. P. *J. Raman Spectrosc*. **1980**, *9*, 247−256.
(44) Frisch, M. J.; Trucks, G. W.; Schlegel, H. B.; Scuseria, G. E.; Robb, M. A.; Cheeseman, J. R.; Zakrzewski, V. G.; Montgomery, J. A., Jr.; Stratmann, R. E.; Burant, J. C.; Dapprich, S.; Millam, J. M.; Daniels, A. D.; Kudin, K. N.; Strain, M. C.; Farkas, O.; Tomasi, J.; Barone, V.; Cossi, M.; Cammi, R.; Mennucci, B.; Pomelli, C.; Adamo, C.; Clifford, S.; Ochterski, J.; Petersson, G. A.; Ayala, P. Y.; Cui, Q.; Morokuma, K.; Malick, D. K.; Rabuck, A. D.; Raghavachari, K.; Foresman, J. B.; Cioslowski, J.; Ortiz, J. V.; Stefanov, B. B.; Liu, G.; Liashenko, A.; Piskorz, P.; Komaromi, I.; Gomperts, R.; Martin, R. L.; Fox, D. J.; Keith, T.; Al-Laham, M. A.; Peng, C. Y.; Nanayakkara, A.; Gonzalez, C.; Challacombe, M.; Gill, P. M. W.; Johnson, B. G.; Chen, W.; Wong, M. W.; Andres, J. L.; Head-Gordon, M.; Replogle, E. S.; Pople, J. A. *Gaussian 98*, revision A.11; Gaussian, Inc.: Pittsburgh, PA, 1998.
(45) Bürig, H.-B.; Dunitz, J. D. *J. Am. Chem. Soc*. **1987**, *109*, 2924−2926.
(46) Li, X.-Y.; Zgierski, M. Z. *J. Phys. Chem*. **1991**, *95*, 4268−4287.
(47) Herschbach, D. R.; Laurie, V. W. *J. Chem. Phys*. **1961**, *35*, 458−463.
(48) Majoube, M. *J. Raman Spectrosc*. **1985**, *16*, 98−110.
(49) Moskovits, M.; Di Lella, D. P. *J. Chem. Phys.* **1980**, *73*, 6068−6075.
(50) Gao, P.; Weaver, M. J. *J. Phys. Chem*. **1985**, *89*, 5040−5046.
(51) Faria, P. A.; Chen, X.; Lombardi, J. R.; Birke, R. L. *Langmuir* **2000**, *16*, 3984−3992.
(52) Li, W.-H.; Li, X.-Y.; Yu, N.-T. *Chem. Phys. Lett*. **1999**, *305*, 303−310.
(53) Vekatesan, S.; Erdheim, G.; Lombardi, J. R.; Birke, R. L. *Surf. Sci.* **1980**, *101*, 387.
(54) Anderson, A. B.; Kotz, R.; Yeager, E. *Chem Phys. Lett*. **1981**, *82*, 130.
(55) Lin, W. F.; Tian, Z. Q.; Sun, S. G.; Tian, Z. W. *Electrochim. Acta* **1992**, *37*, 211−213.
(56) Takahasi, H.; Mamola, K.; Plyler, E. K. *J. Mol. Spectrosc*. **1966**, *21*, 217−230.
(57) Arenas, J. F.; Woolley, M. S.; López Tocón, I.; Otero, J. C.; Maecos, J. I. *J. Chem. Phys*. **2000**, *112*, 7669−7683.
(58) Carter, D. A.; Pemberton, J. E.; Woelfel, K. J. *J. Phys. Chem*. **1998**, *102*, 9870−9880.
(59) Watanabe, T.; Kawanami, O.; Honda, K.; Pettinger, B. *Chem. Phys. Lett*. **1983**, *102*, 565−569.
(60) Bosnick, K. A. Ph.D. Thesis, University of Toronto, 2000.
(61) Haslett, T. L.; Bosnick, K. A.; Moskovits, M. *J. Chem. Phys.* **1998**, *108*, 3453−3457.
(62) Eachus, R. S.; Symons, M. C. R. *J. Chem. Soc. A* **1970**, 1329.
(63) Baetzold, R. C. *J. Chem. Phys.* **1971**, *55*, 4363−4370.
(64) Lambert, D. K. *Electrochim. Acta* **1996**, *5*, 623−630.
(65) Lombardi, J. R.; Birke, R. L.; Lu, T.; Xu, J. *J. Chem. Phys.* **1986**, *84*, 4147−4180.
(66) Moskovits, M. *Rev. Mod. Phys.* **1985**, *57*, 783−826.
(67) Tian, Z. Q.; Li, W. H.; Qiao, Z. H.; Lin, W. F.; Tian, Z. W. *Russ. J. Electrochem*. **1995**, *31*, 935−940. From *Elektrokhimiya* **1995**, *31*, 1014−1020.